Luminescence Color Tuning by Regulating Electrostatic Interaction for Light-Emitting Device and Two-Photon Excited Information Decryption

Yun Ma,[†] Shujuan Liu,[‡] Huiran Yang,[‡] Yi Zeng,[†] Pengfei She,[‡] Nianyong Zhu,[†] Cheuk-Lam Ho,[†] Qiang Zhao,*[,‡] Wei Huang,[‡] and Wai-Yeung Wong*[,†,⊥]

[†] Institute of Molecular Functional Materials, Department of Chemistry and Institute of Advanced Materials, Hong Kong Baptist University, Waterloo Road, Kowloon Tong, Hong Kong, P. R. China

[‡] Key Laboratory for Organic Electronics & Information Displays (KLOEID) and Institute of Advanced Materials (IAM), Nanjing University of Posts & Telecommunications (NUPT), 9 Wenyuan Road, Nanjing 210023, Jiangsu, P. R. China

[⊥] Department of Applied Biology and Chemical Technology, The Hong Kong Polytechnic University, Hung Hom, Hong Kong, P. R. China

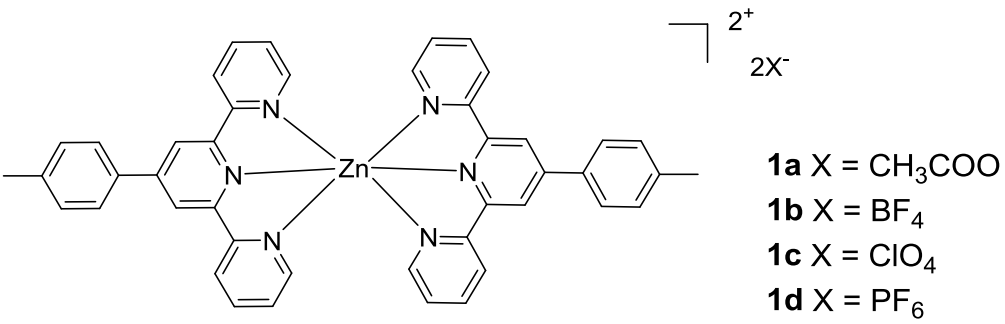

Scheme S1. Chemical structures of model Zn(II) complexes.

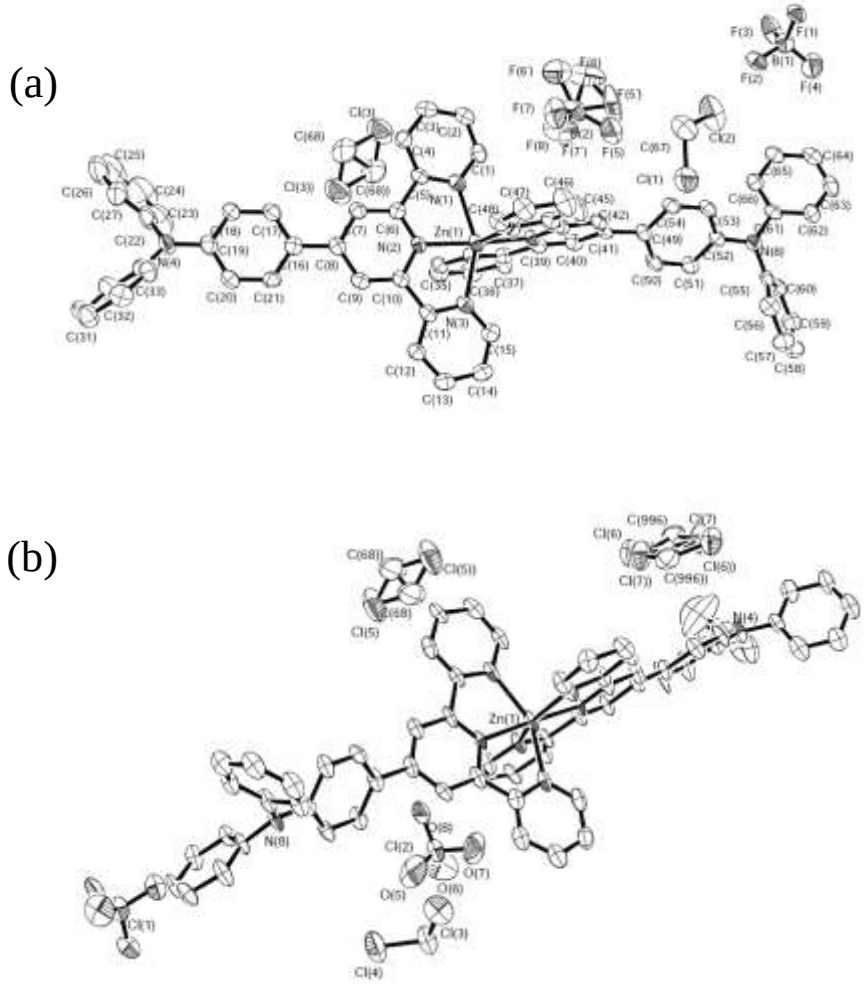

Figure S1 Single-crystal structures of (a) **Zn-BF_4** and (b) **Zn-ClO_4**.

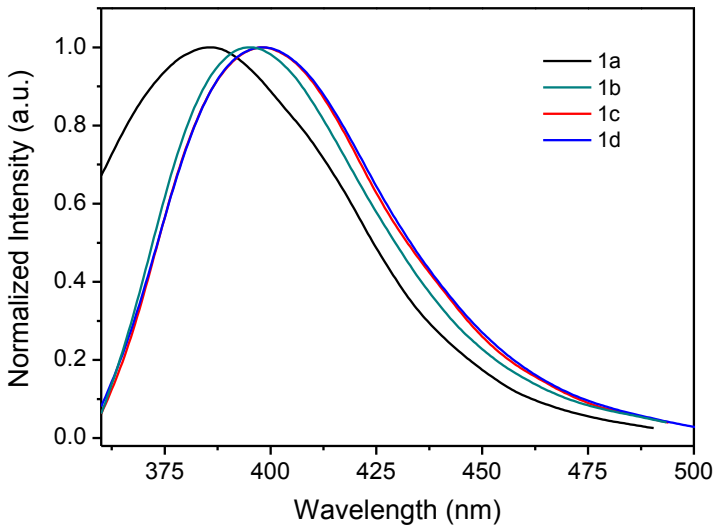

Figure S2 Normalized PL spectra of **1a-1d** in CH_2Cl_2 (10 μM) at room temperature (excitation at 350 nm).

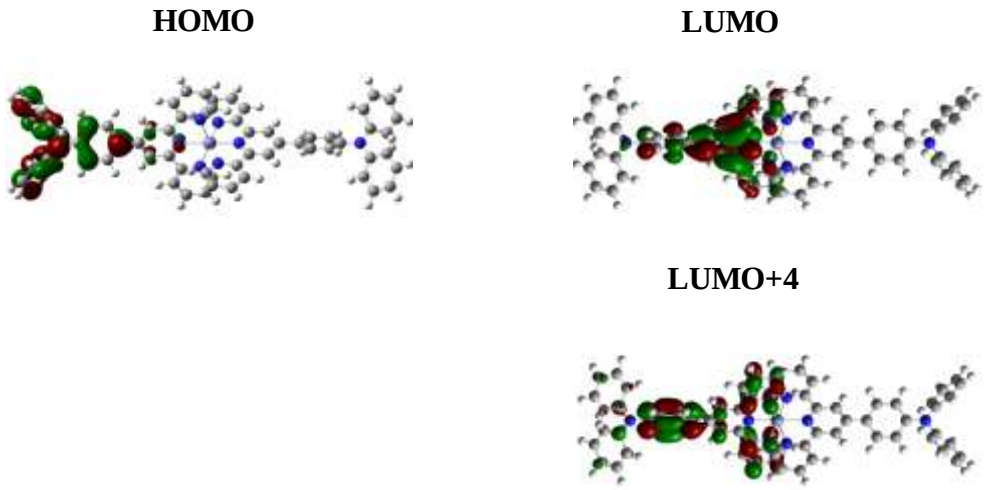

Figure S3 HOMO and LUMO distributions of the cation of the Zn(II) complexes.

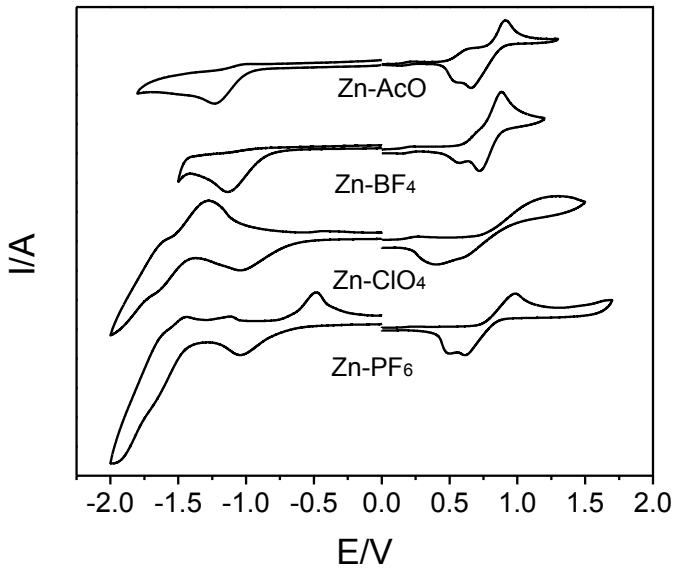

Figure S4 Cyclic voltammograms of complexes **Zn-AcO, Zn-BF_4, Zn-ClO_4** and **Zn-PF_6.**

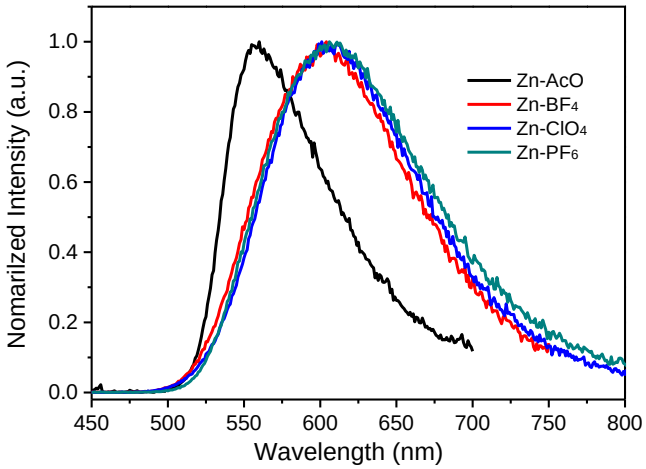

Figure S5 Normalized PL spectra of Zn(II) complexes in the solid state. The emission peaks are located at 560 nm, 604 nm, 601 nm, 606 nm and their quantum efficiencies are 16%, 19%, 21% and 8%, respectively.

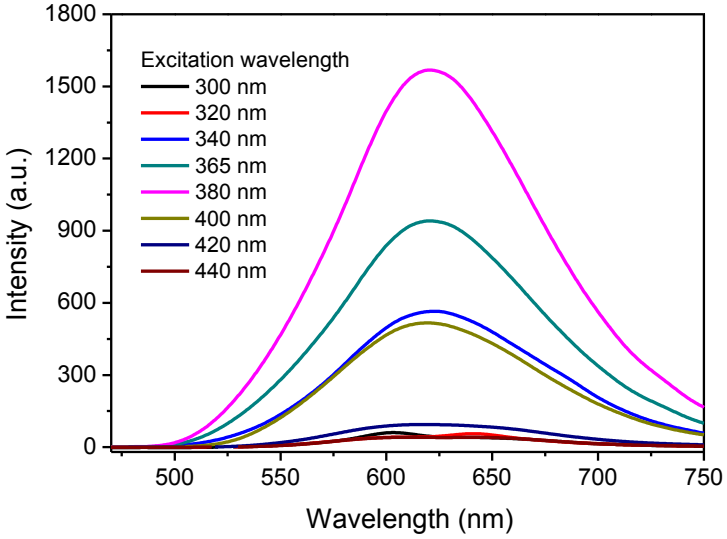

Figure S6 PL spectral change of **Zn-PF_6** (10 μM) under different excitation wavelengths in CH_2Cl_2 solution.

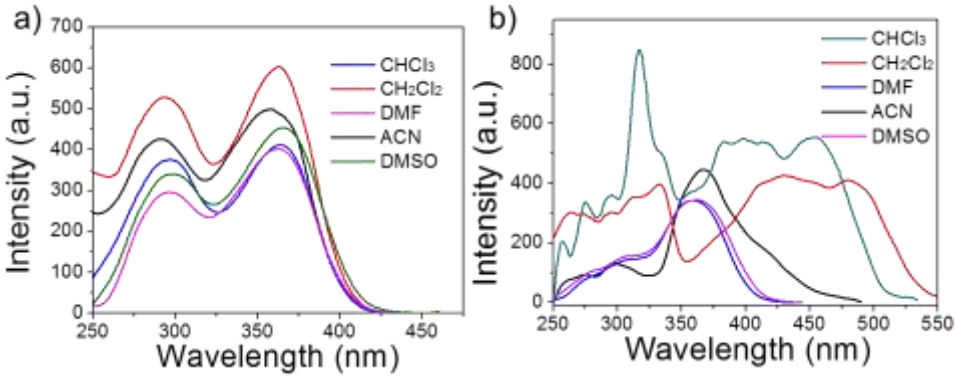

Figure S7 The excitation spectra (10 μM) of (a) ligand and (b) **Zn-PF_6.**

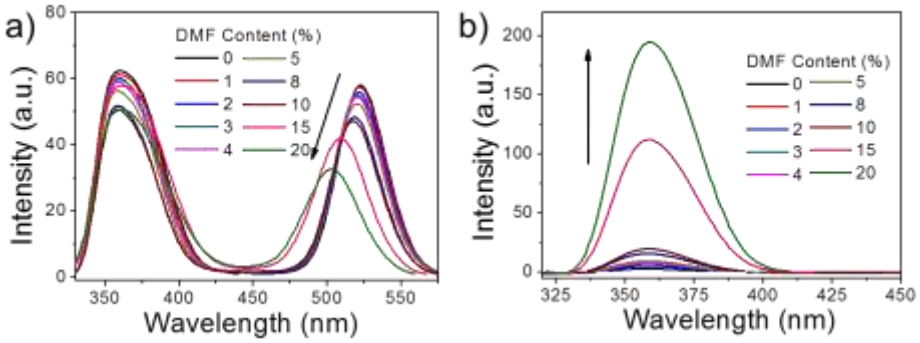

Figure S8 The excitation spectra of **Zn-PF_6** monitored at (a) 622 nm and (b) 500 nm in CH_2Cl_2/DMF mixtures (50 μM) with different DMF fractions.

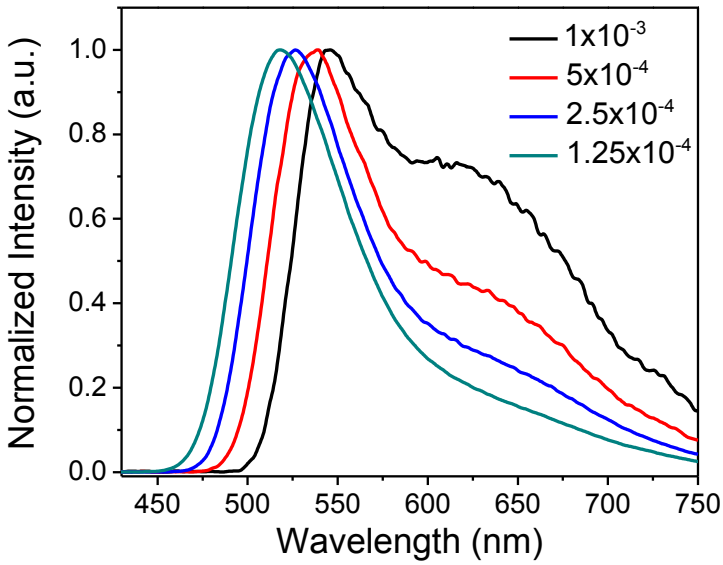

Figure S9 Normalized emission spectra of **Zn-PF_6** in CH_3CN at different concentrations.

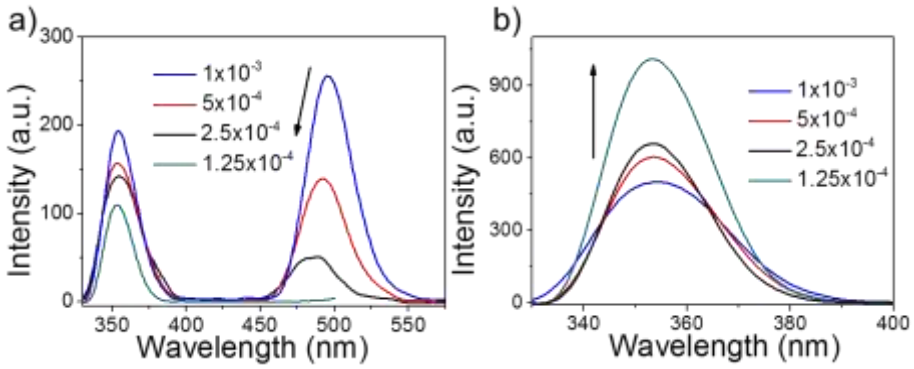

Figure S10 The excitation spectra of **Zn-PF_6** monitored at (a) 622 nm and (b) 500 nm in CH_3CN with different concentrations.

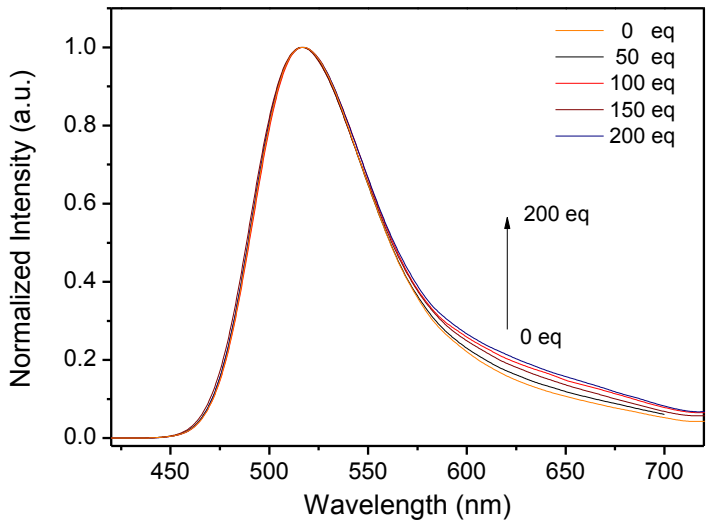

Figure S11 PL spectral change of **Zn-PF_6** (50 μM) after the addition of different amount of $Bu_4N^+PF_6^-$ in DMF solution.

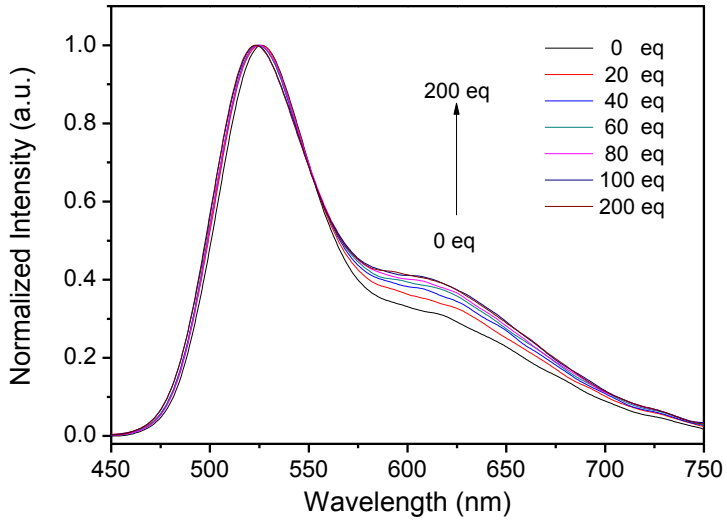

Figure S12 PL spectral change of **Zn-PF_6** (50 μM) after the addition of different amount of $Bu_4N^+PF_6^-$ in CH_2Cl_2/DMF mixture (v/v, 9/1).

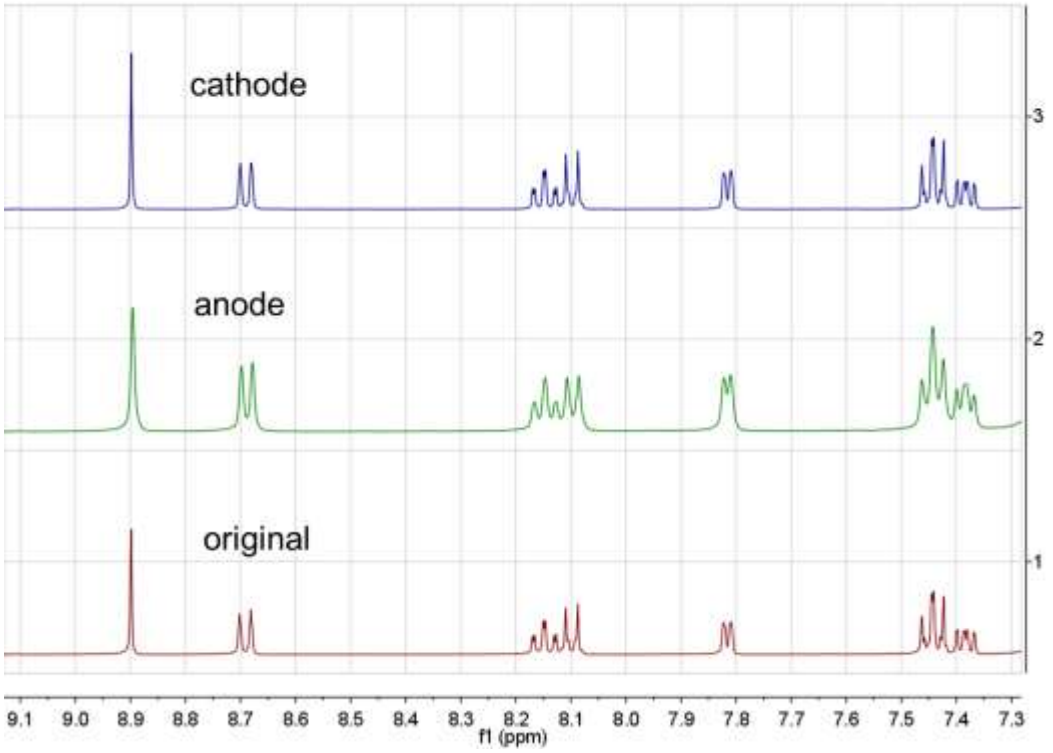

Figure S13 ^{1}H NMR spectra of **Zn-PF$_6$** in CD_3CN during the electrochromic luminescence experiment.

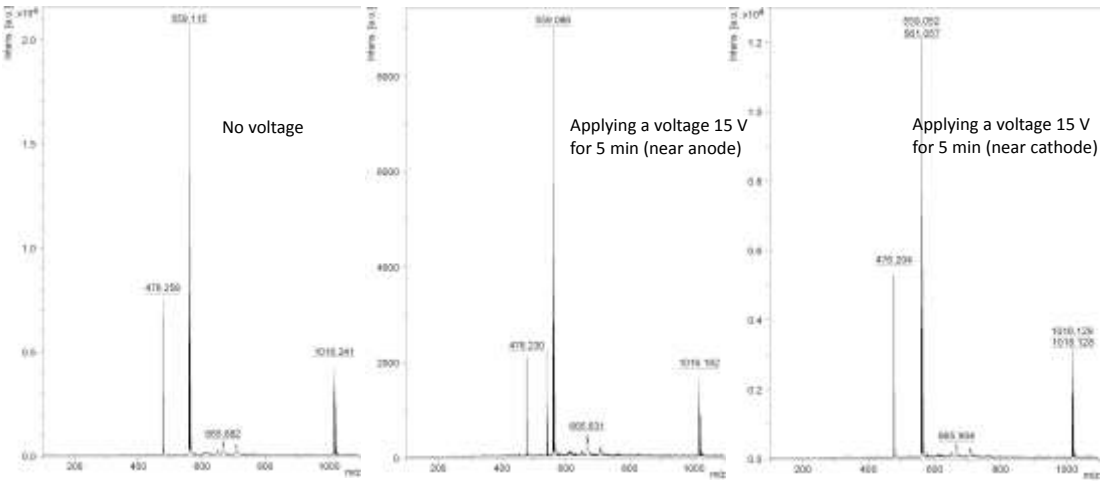

Figure S14 Mass spectra of **Zn-PF_6** in CH_3CN during the electrochromic luminescence experiment.

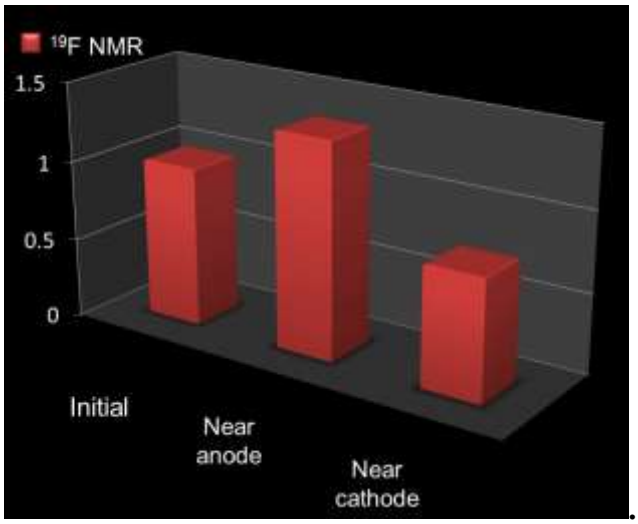

Figure S15 Concentration variation of PF_6^- based on the ^{19}F NMR spectral data during the electrochromic luminescence experiment.

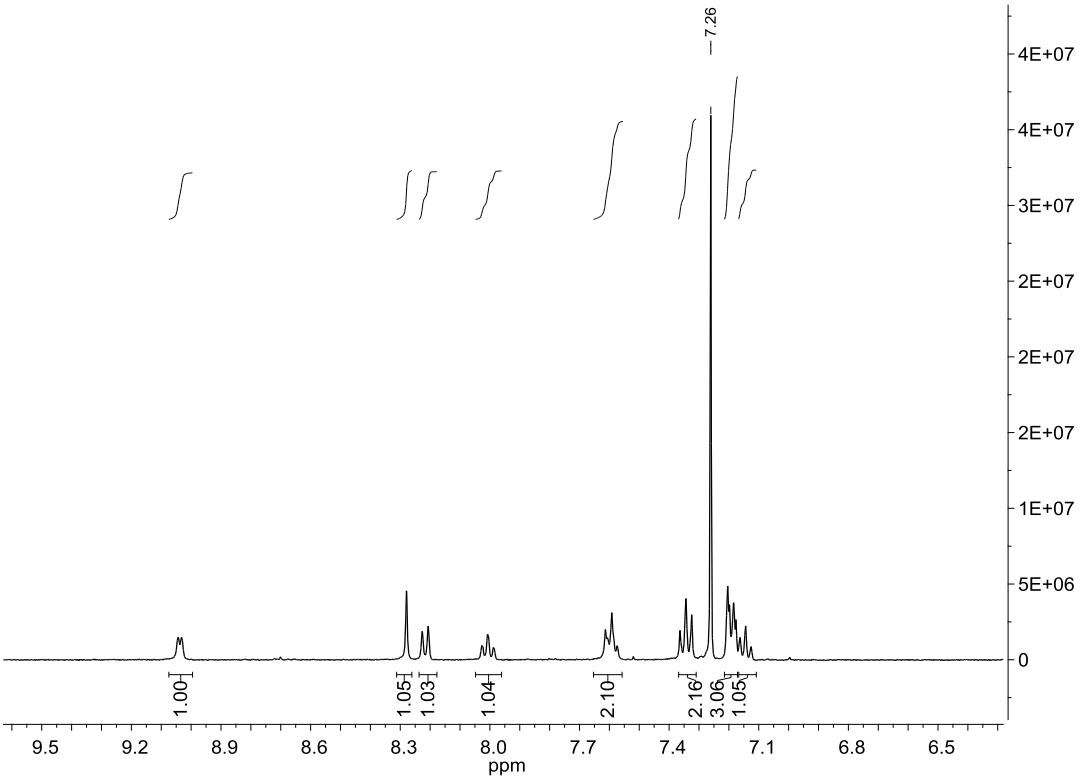

Figure S16 ^{1}H NMR spectrum of **Zn-AcO** in $CDCl_3$.

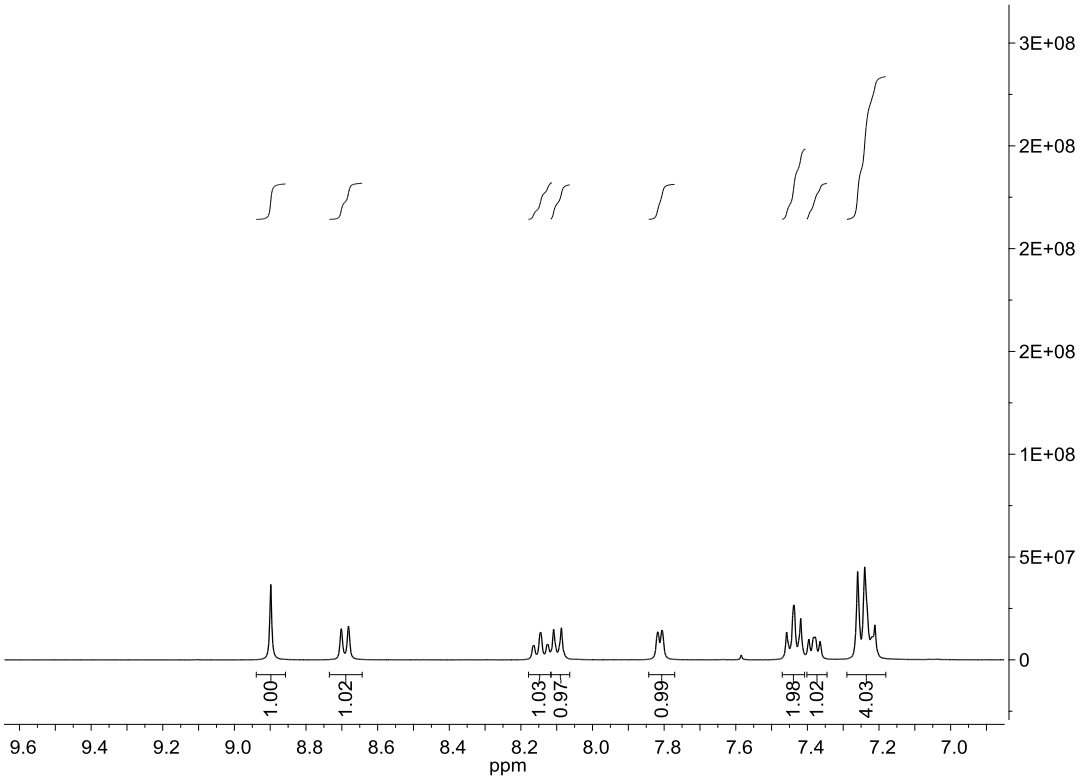

Figure S17 ^{1}H NMR spectrum of **Zn-BF_4** in CD_3CN.

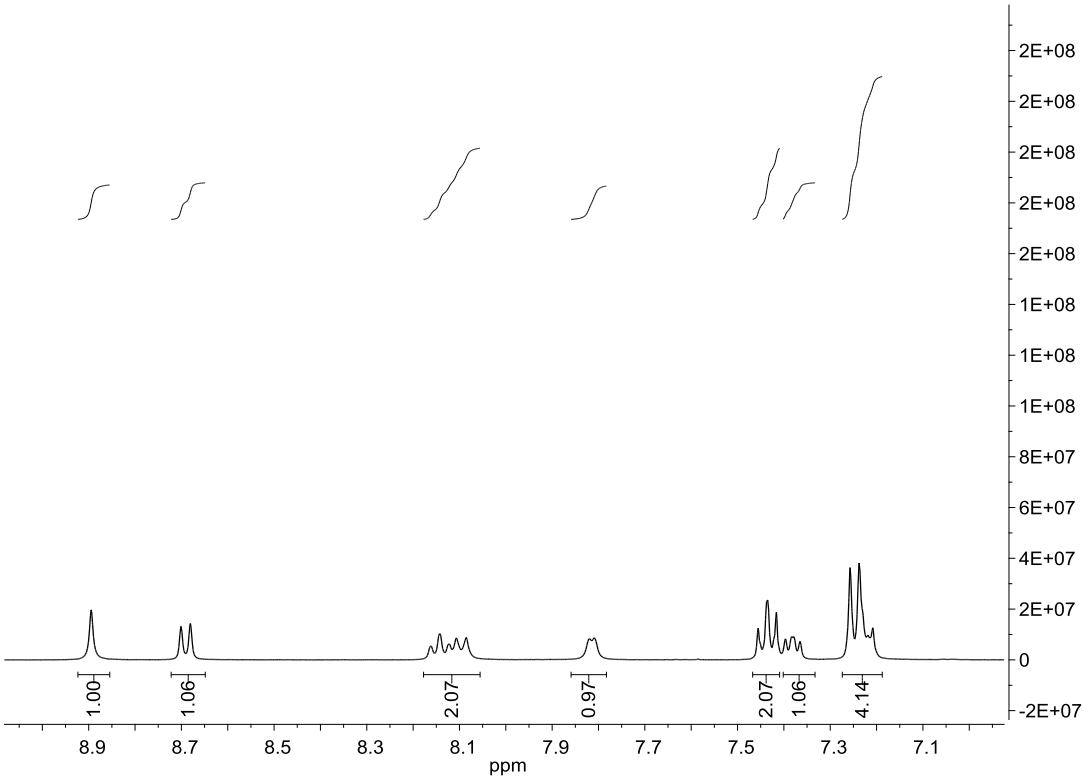

Figure S18 ^{1}H NMR spectrum of **Zn-ClO$_4$** in CD_3CN.

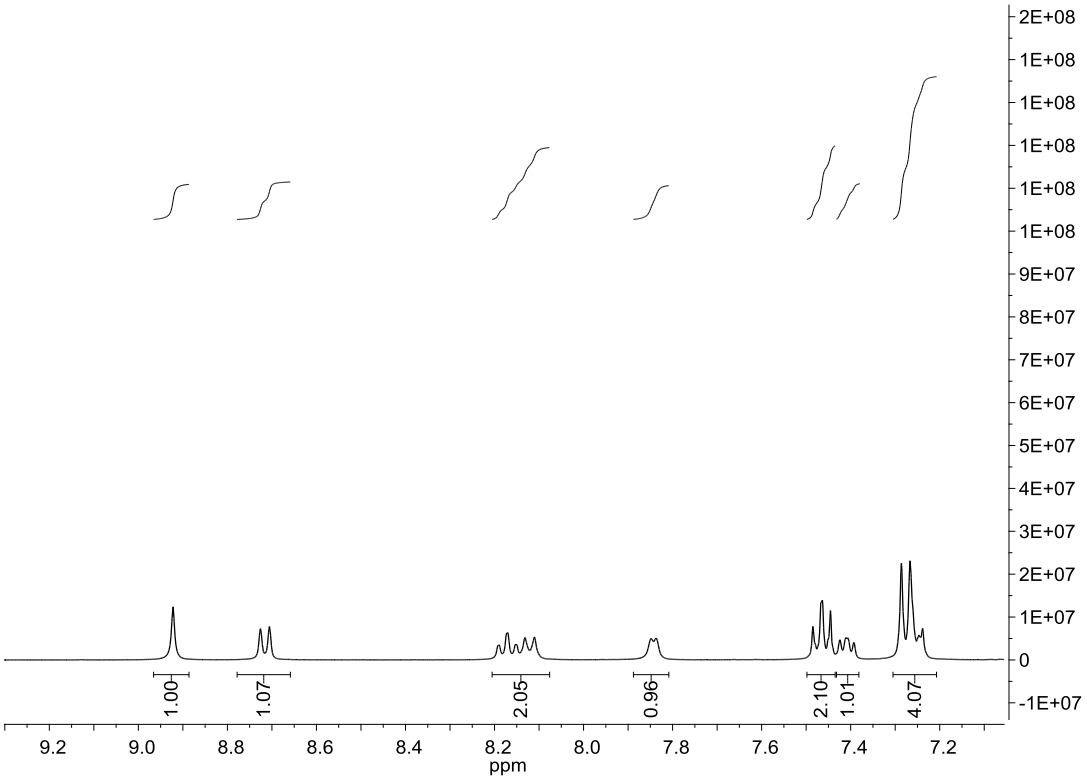

Figure S19 ^{1}H NMR spectrum of **Zn-PF$_6$** in CD_3CN.

Table S1 Summary of X-ray crystallographic data for complexes **Zn-BF_4, Zn-ClO_4** and **Zn-PF_6.** The data for **Zn-ClO_4** are not very accurate due to the poor data set collected and only listed for comparison

Complex	**Zn-BF_4**	**Zn-ClO_4**	**Zn-PF_6**
Empirical Formula	$C_{67.5}H_{51}Cl_3B_2F_8N_8Zn$	$C_{68}H_{52}Cl_6N_8O_8Zn$	$C_{66}H_{48}F_{12}N_8P_2Zn$
Formula Weight	1319.50	1387.24	1308.43
Crystal System	Triclinic	Triclinic	Monoclinic
Space Group	*P*-1	*P*-1	$P2_1/c$
a (Å)	9.194(4)	9.341(3)	10.684(2)
b (Å)	17.447(8)	17.194(7)	16.579(3)
c (Å)	19.681(9)	20.094(8)	36.027(7)
α (^{o})	99.85(4)	98.23(2)	90
β (^{o})	102.05(4)	101.14(2)	91.11
γ (^{o})	91.84(4)	90.71(2)	90
V (Å^3)	3034(2)	3131(2)	6380
Z value	2	2	4
D(calcd) (g cm^{-3})	1.444	1.471	1.362
Temperature (K)	173(2)	173(2)	173(2)
μ (mm^{-1})	2.410	3.430	1.716
F(000)	1350	1424	2672
R_1,wR_2 [I>2σ(I)]	0.0854, 0.2234	0.1401, 0.3711	0.0558, 0.1360

R indices (all data)	0.1049, 0.2393	0.1826, 0.4042	0.0710, 0.1435
Goodness-of-fit on F^2	1.009	1.738	1.042

Table S2 Selected bond lengths [Å] in single crystal structures of **Zn-BF_4**, **Zn-ClO_4** and **Zn-PF_6.**

Zn-BF_4	Zn(1)-N(6)	2.070(4)
	Zn(1)-N(2)	2.071(4)
	Zn(1)-N(1)	2.182(4)
	Zn(1)-N(3)	2.191(4)
	Zn(1)-N(7)	2.199(4)
	Zn(1)-N(5)	2.204(4)
Zn-ClO_4	Zn(1)-N(2)	2.106(6)
	Zn(1)-N(6)	2.107(5)
	Zn(1)-N(3)	2.178(6)
	Zn(1)-N(7)	2.187(8)
	Zn(1)-N(1)	2.202(7)
	Zn(1)-N(5)	2.203(8)
Zn-PF_6	Zn(1)-N(6)	2.054(4)
	Zn(1)-N(2)	2.056(4)
	Zn(1)-N(3)	2.151(4)
	Zn(1)-N(7)	2.155(5)
	Zn(1)-N(1)	2.165(4)
	Zn(1)-N(5)	2.172(4)

Table S3 Photophysical properties of all Zn(II) complexes in CH_2Cl_2 (10 μM) and solid state.

Complex	λ_{abs} (nm)[a]	λ_{PL} (nm)[a]	τ (ns)[a]	Φ_{em}[a]	λ_{PL} (nm)[b]	Φ_{em}[b]
Zn-AcO	284, 302, 407	549	1.85	0.26	560	0.16
Zn-BF_4	284, 321, 334, 457	576	1.67	0.19	604	0.19
Zn-ClO_4	284, 321, 333, 456	594	1.31	0.16	601	0.21
Zn-PF_6	284, 319, 332, 458	622	1.19	0.13	606	0.08

[a] in CH_2Cl_2 [b] in solid state

Table S4 Photophysical properties of **Zn-PF_6** in CH_2Cl_2, $CHCl_3$, CH_3CN, DMSO and DMF (10 μM).

Solvent	Polarity index	λ_{abs}, nm	λ_{PL}, nm	τ, ns	Φ_{em}
CH_2Cl_2	3.4	284, 319, 332, 458	622	1.19	0.13
$CHCl_3$	4.4	286, 320, 335, 453	540	3.82	0.34
CH_3CN	6.2	285, 316, 329, 424	498	5.24	0.06
DMSO	7.2	285, 329, 364, 424	497	6.25	0.43
DMF	6.4	285, 334, 364, 422	489	5.45	0.48

Table S5 Emission wavelengths of **Zn-AcO, Zn-BF_4 and Zn-ClO_4** in CH_2Cl_2, $CHCl_3$, CH_3CN, DMSO and DMF (10 μM).

	Zn-AcO	**Zn-BF_4**	**Zn-ClO_4**
CH_2Cl_2	549 nm	576 nm	594 nm
$CHCl_3$	522 nm	521 nm	528 nm
CH_3CN	495 nm	497 nm	498 nm
DMSO	497 nm	497 nm	496 nm
DMF	491 nm	491 nm	491 nm

Table S6 Photophysical properties of ligand in CH_2Cl_2, $CHCl_3$, CH_3CN, DMSO and DMF (10 μM).

Solvent	λ_{PL}, nm	τ, ns
CH_2Cl_2	473	4.17
$CHCl_3$	454	3.31
CH_3CN	498	4.78
DMSO	504	5.90
DMF	492	5.09

Table S7 Electrochemical data for **Zn-AcO, Zn-BF_4, Zn-ClO_4** and **Zn-PF_6.**[a]

Complex	E_{onset}^{red} (V)	E_{onset}^{ox} (V)
Zn-AcO	-0.96	0.72
Zn-BF_4	-0.87	0.72
Zn-ClO_4	-0.75	0.72
Zn-PF_6	-0.61	0.72

[a] Electrochemical data were obtained in a typical three-electrode cell with a working electrode (glassy carbon electrode), a reference electrode [Ag/Ag^+], referenced against ferrocene/ferrocenium couple, and a counter electrode (Pt wire) under a nitrogen atmosphere at a sweeping rate of 100 mV s^{-1} in a solution of 0.1 M tetra-*n*-butyl-ammounium hexafluorophosphate ($^tBu_4NPF_6$) in CH_2Cl_2. The oxidation profiles are reversible, while the reduction profiles are irreversible.

Table S8 TPA cross sections of complex **Zn-PF_6** and BODIPY.

Wavelength (nm)	BODIPY	**Zn-PF_6 (CH_2Cl_2)**	**Zn-PF_6 (DMF)**
700	4.9	4.3	43.5
720	3.1	8.2	27.9
740	6.2	9.3	22.8
760	4.7	9.2	14.9
780	2.9	22.4	11.6
800	2.7	43.2	9.4
830	3.5	67.6	5.3
850	4	90.8	4.1
870	4.9	96	4.7
890	7.4	81.2	3.5
910	4.9	145.8	2.9
930	7.4	264.8	2.2
950	7.49	298.1	2.7
970	-	229.4	-